Electronic Supplementary Material (ESI) for Lab on a Chip

Supplementary Information: A Method for Non-Invasive Full-Field Imaging and Quantification of Chemical Species

Viktor Shkolnikov, Juan G. Santiago

Department of Mechanical Engineering, Stanford University, Stanford CA, USA

We here present additional information on the following topics:

SI 1. Additional potential SAFI dyes

Here we present a table of 19 additional potential SAFI dyes that have been shown to be quenched by chlorine, bromine, iodine and other anions. Furthermore, these dyes remain electrically neutral between pH 0 and 12 [1] and Krapf et al. and Huber et al. have demonstrated that these dyes have excellent solubility and high quantum yield [2,3].

Table S1. SPQ and SAB analogs which are promising SAFI dyes and their key properties. All dyes, other than the last on this list are from Krapf et al.[2].

Dye	λ_{ex} (nm)	λ_{em} (nm)	Aq. Sol. (M)	Relative Intensity[1]	K_Q Cl- (M^{-1})	K_Q Br- (M^{-1})	K_Q I- (M^{-1})
N-(3-Sulfopropyl)quinolinium	328	400	0.90	0.75	55	73	96
N-(4-Sulfobutyl)quinolinium	322	400	1.20	0.56	59	81	111
N-(3-Sulfopropyl)isoquinolinium	336	380	1.00	1.62	36	124	163
N-(4-Sulfobutyl)isoquinolinium	336	376	1.73	1.64	26	123	179
N-(3-Sulfopropyl) phenantridinium	368	406	0.003	0.61	25	87	120
N-(3-Sulfopropyl)-(5,6-benzyl)quinolinium	372	434	0.004	1.64	3	80	106
N-(3-Sulfopropyl)-(7,8-benzyl)quinolinium	370	434	0.01	1.09	3	68	110
6-Methodxy-*N*-(4-Sulfobutyl) quinolinium	350	440	0.43	0.98	78	154	233
6-Methyl-*N*-(3-Sulfopropyl) quinolinium	355	410	0.08	0.77	83	123	171
2-Methyl,6-Methoxy-*N*-(3-Sulfopropyl)quinolinium	346	436	0.54	0.86	26	134	180
3-Bromo-*N*-(3-Sulfopropyl) quinolinium	330	426	0.18	0.16	3	75	109
3-Chloro-*N*-(3-Sulfopropyl) quinolinium	322	406	0.14	0.13	11	15	26
2-Methyl-*N*-(3-Sulfopropyl) quinolinium	324	428	0.51	-[3]	73	102	141
4-Methyl-*N*-(3-Sulfopropyl) quinolinium	345	400	0.11	1.63	87	118	156
7-Methyl-*N*-(3-Sulfopropyl) quinolinium	334	406	0.16	1.30	76	149	199
8-Methyl-*N*-(3-Sulfopropyl) quinolinium	336	484	0.17	-[3]	59	177	204
2,6-Dimethyl-*N*-(3-Sulfopropyl) quinolinium	320	406	0.28	0.96	97	148	213
2,6-Dimethyl-*N*-(4-Sulfobutyl) quinolinium	330	406	0.25	0.82	90	148	224
N,N-Di-(3-Sulfopropyl)-9,9-bisacridinium[2]	460	515	-[3]	-[3]	124	209	271

[1] Relative to SPQ; all dye concentrations were 0.1 mM.
[2] From Huber et al. [3]; for this dye K_Q was measured in 5 mM phosphate buffer. Additionally Werner et al. found that this dye exhibits Stern-Volmer type quenching for fluoride, nitrate, sulfate, phosphate, and common buffers 3-(*N*-morpholino)propanesulfonic acid (MOPS) and *N*-2-hydroxy-ethylpiperazine-*N*′-ethansulfonic acid (HEPES)[4]. All other dyes from Krapf et al.[2]; for these dyes K_Q was measured in 5 mM HEPES/Tris pH 7.4 buffer. Note that HEPES and Tris ions also are likely contribute to the quenching of fluorescence.
[3] Not reported

SI 2. Species concentration quantitation in special cases using Stern-Volmer quenching

We further describe quantitation of solutions where some information about solution composition is known a priori. In our work, we analyzed five main cases: Case 0 describes quantification of a solution consisting of a single acid and a single base; Case 1 solutions where the relative ratios of all quenching species are expected to remain invariant; Case 2 describes flow with two regions in space, one with a set of analytes whose concentrations remain invariant and a second containing a set of analytes whose relative ratios are expected to remain invariant; and Case 3 describing a single region of the flow containing two sets of species (one set of known, fixed concentration and a second with fixed relative concentration ratios). Each of these cases allows us to significantly reduce the number of dyes and calibration experiments needed to quantify solution composition. In the main text, we described Cases 1 and 2. Here we expand on descriptions of the other two cases, Cases 0 and 3.

For the special case (Case 0) of a solution consisting of a single acid and a single base we need only three SAFI dyes to quantify n species present in solution. In the ideal case (no complexation between acid derivatives and base derivatives), the species in solution would consist of the undissociated acid, j acid derivatives (corresponding to j ionization states), the undissociated base, and k base derivatives (again corresponding to k ionization states). Thus, there are $n = j + k + 2$ species in solution (excluding hydronium and/or hydroxide ions). For this case we would have $j + k$ acid-base equilibrium equations and two species conservation equations. Since the pH and total concentrations of the acid and the base would also be unknown (for a total of $n + 3$ unknowns), we would need three Stern-Volmer equations and therefore three dyes to obtain both the concentrations of all species present in solution and the solution pH. We would of course require a calibration of n quenching constants for each of the three SAFI dyes. As an example, suppose we wish to quantify endogenous species concentrations of region containing a solution of acetic acid and Tris. Acetic acid and Tris have each only one dissociation constant between pH 0 and 12 [5]. Therefore, in this pH range, the solution may contain the acetate anion, neutral acetic acid, Tris cation, and neutral Tris base for a total of $n = 4$ species. We thus need to calibrate the quenching constant for each of these species for three dyes, for a total of 12 quenching constants. We then can simultaneously solve the respective equations (2) (of the main text) for each of the three dyes together with acid base equilibrium equations for acetic acid and Tris and obtain the concentrations of all $n = 4$ species in solution and the local pH.

Recall that Case 1 and Case 2 are described in Section 2.2 of the main text.

Another special case (Case 3) is where we consider two sets of species. The first set of species has concentrations which remain invariant in the entire flow field. In the second set, the concentration of species varies but the relative concentration ratios of this second set are invariant. Here again, as in Case 2, we only need a single dye and a single quenching constant to quantify concentrations of all quenching species present. As an example, we encounter this case in the EKI experiment we describe in Section 4.3 of the main text. Here, the solution pH and the concentration of buffering HEPES remain invariant while the concentration of potassium chloride varies in flow field. For this case, we write equation (2) (main text) as

$$\frac{F_0}{F} = 1 + K_{Q,e,inv} c_{inv} + K_{Q,e,var} c_{var}, \qquad (1)$$

where $K_{Q,e,inv}$ is the effective quenching constant of the species whose concentrations remain invariant, c_{inv} is that invariant concentration, $K_{Q,e,var}$ is the effective quenching constant of the species whose concentrations change, but whose ratio remains the same, and c_{var} is the concentration of the species for which $K_{Q,e,var}$ was calibrated. By definition, the product $K_{Q,e,inv}c_{inv}$ is constant. To quantify the concentrations of species whose concentrations (proportional to c_{var}) changes in the flow field, we need only measure $K_{Q,e,var}$. We can measure this by measuring the F_0/F ratio as a function of c_{var} and fitting this to equation (1). The slope of this fit provides $K_{Q,e,var}$ and the intercept with the ordinate provides $1+K_{Q,e,inv}c_{inv}$. Lastly, we need an internal reference point for the concentration field of c_{var}, $c_{var,1}$. This reference point may be, for example, an inlet flow where the concentration c_{var} is known *a priori*. From, equation (1) rearanged as

$$c_{var,2}=\frac{1}{K_{Q,e,var}}\left[\frac{F_1}{F_2}\left(1+K_{Q,e,inv}c_{inv}+K_{Q,e,var}c_{var,1}\right)-\left(1+K_{Q,e,inv}c_{inv}\right)\right]. \qquad (2)$$

Here the subscripts 1 and 2 denote respectively the known reference value of c_{var} and the unknown concentration values.

We can define the sensitivity of quantification using Case 3 as was done for Case 1 in the main text (Section 2.3). We again define the sensitivity as the partial derivative of florescence intensity with concentration. Taking this derivative of equation (1) we obtain

$$\frac{\partial F}{\partial c_{var}}=\frac{-F_0K_{Q,e,var}}{\left(1+K_{Q,e,inv}c_{inv}+K_{Q,e,var}c_{var}\right)^2}. \qquad (3)$$

Here again the sensitivity, $\partial F/\partial c_{var}$ is proportional to F_0, and thus proportional to the concentration of dye and excitation illumination intensity. Here when the product $K_{Q,e,var}c_{var}$ is sufficiently greater than $1+K_{Q,e,inv}c_{inv}$ we see the sensitivity $\partial F/\partial c_{var}$ scales as $-F_0/K_{Q,e,var}c_{var}{}^2$. On the other hand, where the product $K_{Q,e,var}c_{var}$ is sufficiently smaller than $1+K_{Q,e,inv}c_{inv}$, the sensitivity scales as $-F_0K_{Q,e,var}\left/\left(1+K_{Q,e,inv}c_{inv}\right)^2\right.$. Thus, the behavior is very similar to the sensitivity of Case 1. When measuring relatively high analyte concentrations, the effective quenching constant for the analytes should be small. On the other hand, when measuring low analyte concentration, the effective quenching constant for the analytes should large, and the concentration and quenching constant of the species whose concentration does not change should be as small as possible.

SI 1.2 Method resolution for Stern-Volmer quenching

We define concentration resolution of the SAFI method as the difference in fluorescence intensity between zones of different composition. For Case 2 in the main text, the difference in

fluorescence intensity between the zones of different composition, $F_2 - F_1$, can be obtained from equation (3) (main text) evaluated in each zone. (Note that dye fluorescence intensity in absence of quenchers F_0 should be the same in both zones).

$$F_2 - F_1 = F_0 \left(\frac{K_{Q,e,1}c_1 - K_{Q,e,2}c_2}{1 + K_{Q,e,1}c_1 + K_{Q,e,2}c_2 + K_{Q,e,1}c_1 K_{Q,e,2}c_2} \right), \quad (4)$$

where the subscript 1 or 2 refers to the corresponding zone. Equation (4) can be used to estimate whether the zone boundaries can be observed for the expected concentrations of analytes and a given the resolution of the detector. We see that resolution is improved by increasing the base value F_0 and the difference $K_{Q,e,1}c_1 - K_{Q,e,2}c_2$.

SI 3. Details of anionic ITP experiments

We performed anionic ITP experiments according to the procedure described in Section 3.2.2 of the main text. For anionic ITP visualized with SPQ (Figure 4a of the main text), the solution composition was as follows:

LE	20 mM HCl
	40 mM Tris
	1% PVP
	5 mM SPQ
TE + analytes	10 mM $NaNO_2$
	20 mM 3,5 dinitrobenzoate sodium
	100 mM HEPES
	200 mM Tris
	1% PVP
pure TE	100 mM HEPES
	200 mM Tris
	1% PVP.

For anionic ITP visualized with SAB (Figure 4b of the main text) solution, the composition was as follows:

LE	50 mM Formic Acid
	100 mM Tris
	1% PVP
	2 mM SAB
TE + analytes	10 mM Nicontinic
	10 mM HEPES;
	50 mM L-Asperagine
	100 mM Tris
	1% PVP
pure TE	50 mM L-Asperagine
	100 mM Tris
	1% PVP.

To quantify analyte concentrations in anionic ITP we calibrated SPQ dye according to the procedure described in Section 3.2.1 of the main text. We show the resulting Stern-Volmer plots for quenching of SPQ in Figure S1. We used the quenching constants obtained in these calibrations to quantify the concentrations of analytes in ITP by employing equation (4) of the main text. For the cases of nitrite, carbonic acid, and 3,5-dinitrobenzate, the calibration solutions contained both sodium and Tris as counterion, while in ITP, only Tris served as counterion. For these analytes it is difficult to perform calibrations using binary solutions with Tris as the sole counterion as stock supplies of these chemicals included sodium as the counter ion. We note this as a disadvantage of these endogenous ions, as extraneous counterions may have a significant effect on the quenching constant. We hypothesize that is may be one reason for the discrepancies in published quenching constants for chloride-SPQ pair. For example, Shkolnikov et al. [6] reported this constant to be 107 M^{-1} (sodium chloride solution) which is close to the one obtained here (106 M^{-1}) (Tris chloride solution). On the other hand, Vasseur et al. [7] report this to be 156±6 M^{-1} (potassium chloride), while Krapf et al. [2] report this to be 118 M^{-1} (HEPES-Tris-chloride buffer, pH 7.4). We thus stress that, ideally, quenching constants of analyte buffer ions should be measured with counterions that are going to be used in the actual experiment.

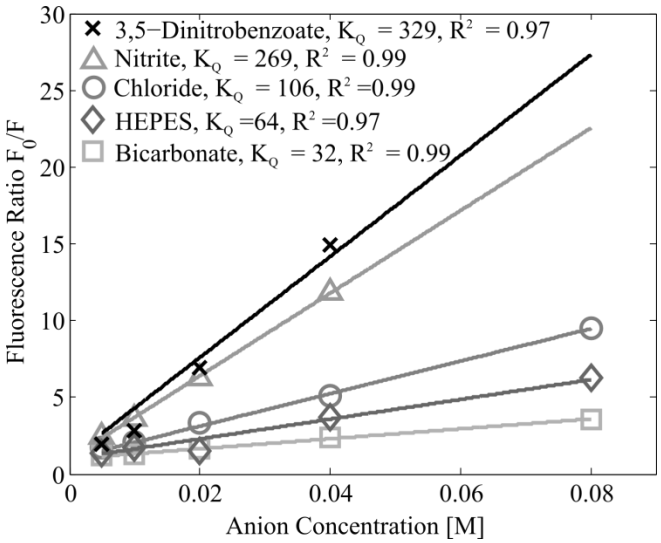

Figure S1. Stern-Volmer plot for quenching of 6-methoxy-N-(3-sulfopropyl) quinolinium (SPQ) by the following four buffers: 3,5-dinitrobenzoate-sodium-Tris (x, pH 10.3), nitrite-sodium-Tris (△, pH 10.3), chloride-Tris (○, pH 8.1), HEPES-Tris (◊, pH 8.4), and sodium bicarbonate-Tris (□, pH 9.4). The regression coefficients R^2 are greater than 0.97 for analyte (anionic buffer component) concentrations from 5 to 80 mM. We note that for nitrite, carbonic acid, and 3,5-dinitrobenzate the calibration solutions contained both sodium and Tris as counterion, while in the ITP process, only Tris served as counterion. For these analytes it is difficult to perform calibrations using binary solutions with Tris as the sole counterion as stock supplies of these chemicals included sodium as the counter ion.

SI 4. Quantifying fluorescence enhancement of SAB dye

10-(3-sulfopropyl)acridinium betaine (SAB) dye exhibited fluorescence enhancement with amediol-HEPES, imidazole-HEPES, pyradine-HEPES, Tris-HEPES, and sodium-HEPES buffers. We plot the fluorescence ratio (dye florescence in absence of buffer to dye fluorescence with buffer present) for 5 to 80 mM buffer concentrations in Figure S2. These buffers exhibited a fluorescence increase with increasing buffer concentration.

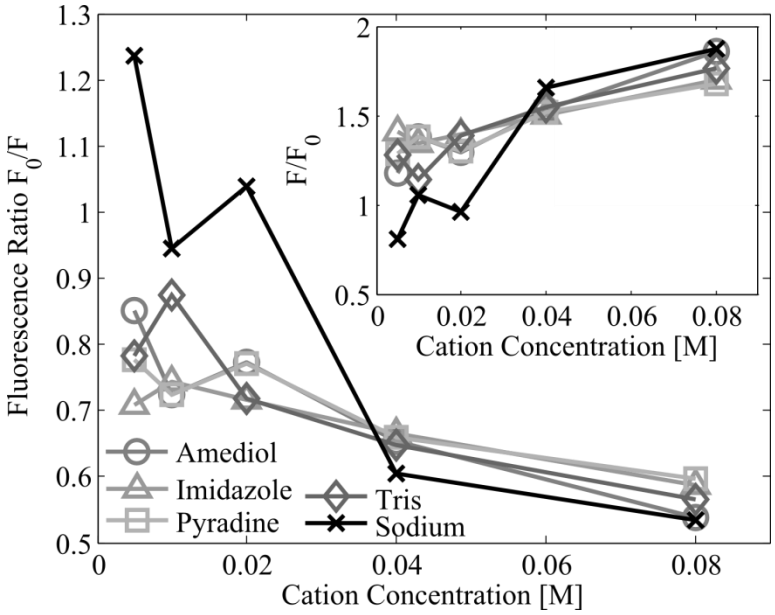

Figure S2. Stern-Volmer plot for quenching of 10-(3-sulfopropyl)acridinium betaine (SAB) by the following four buffers: amediol-HEPES (○, pH 7.4), imidazole-HEPES(△, pH 7.1), pyradine- HEPES (□, pH 6.2), Tris-HEPES (◊, pH 7.3), and sodium-HEPES (x, pH 7.4). Inset: fluorescence intensity in the presence of the buffer scaled by the that in the absence of the buffer. The florescence is in the presence of buffers at almost at concentrations between 5 and 80 mM (except sodium-HEPES) is larger than that in the absence of buffer, indicating fluorescence enhancement.

SI 5. Recommendations regarding dye calibration

We recommend calibrating the quenching constants of analyte-dye pairs near (e.g., within 1 order of magnitude of) the anticipated analyte concentration before performing concentration measurement experiments. These calibration experiments are designed to show whether the analyte-dye pair exhibits Stern-Volmer type quenching and whether the fluorescence quenching or enhancement can be used easily to quantify analyte concentration. If the analyte-dye pair exhibits Stern-Volmer type quenching, the measured quenching constant can be used to predict the sensitivity and/or resolution of the concentration measurements as per analysis in Section 2.3 of the main text.

We further recommend measuring the quenching constant in calibration using the optical detection instrument (including adsorption color filters, illumination source, detector, etc.) to be employed in the flow field measurement of interest. Apparent dye quantum yield is a function of illumination and readout spectra, and thus dependent on the instrument. Traditionally quantum yield for fluorescence is defined as the ratio of number of photons emitted to the number of photons absorbed by the dye [8]. Similarly, we define the apparent quantum yield as the intensity signal measured by the detector (camera) to the absorbable light intensity reaching the sample.

Although not necessary to perform a quantitative SAFI measurement, it is useful to identify the sources of instrument dependence on SAFI visualization signals. We here offer a simple model describing this response in order to highlight the important factors contributing to measured SAFI type signals. The total absorbable light intensity is the product of the light intensity of the light source, the transmission of the excitation filter and the dichroic mirror in our microscope, and the absorption spectra of the dye, summed over all wavelengths. The total signal intensity measured by the detector can be approximated as the product of dye emission spectra, the transmission of the emission filter and the dichoic mirror and the wavelength-dependent sensitivity of the camera, summed of all wavelengths. We thus approximate the expression for apparent quantum yield for a fluorescent dye, Y_0, as

$$Y_0 = \frac{\int_0^\infty I_{emdye}(\lambda) T_{emfilt}(\lambda) T_{dichroic}(\lambda) S_{camera}(\lambda) d\lambda}{\int_0^\infty I_{emlight}(\lambda) T_{exfilt}(\lambda) T_{dichroic}(\lambda) a_{dye}(\lambda) d\lambda}. \quad (5)$$

Here T is the transmission for the optical component, S is the sensitivity of the camera, I is the emitted intensity, and a is the absorption spectra of the dye. Note that these latter four quantities are strong functions of wavelength λ. The subscripts emdye refers to dye emission, emlight to the emission of the light source, emfilt to the emission filter, exfilt the excitation filter, dichroic to the dichroic mirror, and camera to the imaging camera. Similarly, for a fluorescent dye undergoing quenching, the expression for apparent quantum yield, Y can be approximated as

$$Y = \frac{\int_0^\infty q(\lambda) I_{emdye}(\lambda) T_{emfilt}(\lambda) T_{dichroic}(\lambda) S_{camera}(\lambda) d\lambda}{\int_0^\infty I_{emlight}(\lambda) T_{exfilt}(\lambda) T_{dichroic}(\lambda) a_{dye}(\lambda) d\lambda}, \quad (6)$$

where q is a quenching parameter. From equations (5) and (6), we observe that the apparent quantum yield of the dye could be significantly different between different measurement setups if the intensity or spectra of the light source, absorption, transmission, and/or reflectance spectral functions of the optical components, or spectral shape or magnitude of the sensitivity of the

camera are significantly different. Since the observed fluorescence intensity is proportional to the observed quantum yield, we can combine equations (5) and (6) and equation (3) of the main text to obtain for Stern-Volmer quenching

$$\frac{\int_0^\infty I_{emdye}(\lambda)T_{emfilt}(\lambda)T_{dichroic}(\lambda)S_{camera}(\lambda)d\lambda}{\int_0^\infty q(\lambda)I_{emdye}(\lambda)T_{emfilt}(\lambda)T_{dichroic}(\lambda)S_{camera}(\lambda)d\lambda} = 1 + K_{Q,e}c_1. \quad (7)$$

We observe that if the quenching parameter q is a function of wavelength then the Stern-Volmer constant is also a function of wavelength. Some dye-analyte pairs exhibiting Stern-Volmer quenching also exhibit strong wavelength dependence of the Stern-Volmer constant. For example, Chowdhury et al. found a strong, non-linear ($K_{Q,e} \sim \lambda^2$) relationship between the Stern-Volmer constant and dye emission wavelength for nucleic acid intercalating dyes and gold nano-clusters [9]. We note that the discrepancies in quenching constants will lead to discrepancies in measured concentration. For example, for Case 2 in the main text, we find that the percent uncertainty in the measured analyte concentration, $\partial c_2/c_2$, is proportional to the percent uncertainty in the analyte-dye quenching constant, $\partial K_{Q,e,2}/K_{Q,e,2}$:

$$\frac{\partial c_2}{c_2} = -\frac{\partial K_{Q,e,2}}{K_{Q,e,2}}. \quad (8)$$

Thus, the discrepancies in the quenching constant will lead to proportional discrepancies in the concentration for this case. We thus highlight the importance of measuring the quenching constant with the same instrument to be employed in concentration field quantitation.

References

1. ACD/Labs, *Advanced Chemistry Development (ACD/Labs) Software*. 2012.
2. Krapf, R., et al., *Structure-activity relationships of chloride-sensitive fluorescent indicators for biological application.* Analytical Biochemistry, 1988. **169**(1): p. 142-150.
3. Huber, C., et al., *Synthesis and characterization of new chloride-sensitive indicator dyes based on dynamic fluorescence quenching.* J. Photochem. Photobiol. A: Chem., 1999. **128**(1–3): p. 111-120.
4. Werner, T., et al., *Anion-lnduced Fluorescence Quenching of a New Zwitterionic Biacridine Derivative.* Photochemistry and Photobiology, 1999. **70**(4): p. 585-589.
5. Persat, A., R.D. Chambers, and J.G. Santiago, *Basic principles of electrolyte chemistry for microfluidic electrokinetics. Part I: Acid-base equilibria and pH buffers.* Lab on a Chip, 2009. **9**(17): p. 2437-2453.
6. Shkolnikov, V., S.S. Bahga, and J.G. Santiago, *Desalination and hydrogen, chlorine, and sodium hydroxide production via electrophoretic ion exchange and precipitation.* Physical Chemistry Chemical Physics, 2012.

7. Vasseur, M., R. Frangne, and F. Alvarado, *Buffer-dependent pH sensitivity of the fluorescent chloride-indicator dye SPQ.* American Journal of Physiology - Cell Physiology, 1993. **264**(1): p. C27-C31.
8. Lakowicz, J.R., *Principles of Fluorescence Spectroscopy*. 3 ed. 2006, New York: Springer
9. Chowdhury, S., et al., *Wavelength Dependence of the Fluorescence Quenching Efficiency of Nearby Dyes by Gold Nanoclusters and Nanoparticles: The Roles of Spectral Overlap and Particle Size.* The Journal of Physical Chemistry C, 2011. **115**(41): p. 20105-20112.